When and How Much to Neutralize Interference?

Zhao Li*†, Kang G. Shin†, Lu Zhen*
*†State Key Laboratory of Integrated Service Networks, Xidian University
†Department of Electrical Engineering and Computer Science, The University of Michigan
zli@xidian.edu.cn, kgshin@eecs.umich.edu, zhenlu_0320@126.com

***Abstract*—Interference management (IM) is essential to wireless communication networks, but interference suppression, a key component of IM, is known to degrade users' achievable spectral efficiency (SE). It is thus important to select an appropriate IM method with optimal operating parameters according to diverse network deployments, transmit power differences of various communication equipments, and dynamically changing channel conditions so as to balance the benefits brought by and the cost of IM.**

Interference neutralization (IN) has recently been receiving considerable attention, with which a duplicate of interference of the same strength and opposite phase w.r.t. the original interfering signal is generated to neutralize the disturbance at the intended receiver. However, to the best of our knowledge, all existing IN schemes assume that interference is completely neutralized without accounting for their power consumption. To remedy this deficiency, we propose a novel scheme, called *dynamic interference neutralization* (DIN). By intelligently determining the appropriate portion of interference to be neutralized, we balance the transmitter's power used for IN and the desired signal's transmission. We then present a new way to adaptively select one of DIN and other IM methods by taking into account the cost of multiple IM methods and their benefits. Our analysis has shown that DIN can include complete IN and non-interference management (non-IM) as special cases. The proposed strategy is shown via simulation to be able to make better use of the transmit power than existing IM methods, hence enhancing users' SE.

I. Introduction

With the rapid development of wireless communication technologies as well as the increasing density of link connectivity, interference becomes a key impediment in network performance, and thus, interference management (IM) has become a critical issue that warrants a thorough investigation. IM can be implemented at the transmitter and/or the receiver side. There have been numerous IM schemes proposed thus far, such as zero-forcing beamforming (ZFBF) [1], zero-forcing (ZF) reception [2], interference alignment (IA) [3–5], and interference neutralization (IN) [6–12]. They are all designed to suppress, adjust or eliminate interference so as to improve network capacity and users' experience.

Of these IM methods, IA is attractive and under development in recent years [3–5]. By pre-processing them at the transmitter, multiple interfering signals are mapped into a finite subspace, i.e., the overall interference space at the destination/receiver is minimized, so that the desired signal(s) may be sent through a subspace without attenuation. The authors of [4] have shown that the feasibility of IA is highly dependent on system parameters, such as the number of transmitters and receivers and configuration of transmit/receive antennas. IA-based beamforming was proposed in [5] to improve the downlink performance of multiple cell-edge users in multi-user MIMO (Multiple-input multiple-output) systems.

For wireless networks, interference can be not only aligned but also canceled through multiple paths, which is referred to as *interference neutralization* (IN) [6–12]. IN strives to properly combine signals arriving from various paths in such a way that the interfering signals are canceled while the desired signals are preserved [7]. It can be regarded as distributed zero-forcing of interference, i.e., transmissions from separate sources cancel each other at a destination without either source actually forming a null to the destination [8]. The authors of [7] constructed a linear distributed IN scheme that encodes signals in both space and time for separated multiuser uplink-downlink two-way communications. An aligned IN was proposed in [8] for a multi-hop interference network formed by concatenation of two 2-user interference channels. This mechanism provides a way to align interference terms over each hop in such a way to cancel them over the air at the last hop. IN and ergodic IN for multi-source multi-hop networks were reviewed in [9] and [10], respectively, which analyzed the achievable degrees of freedom (DoFs) and approximate capacity. An instantaneous relay (i.e., a relay without delay) was introduced in [11–12] to achieve a higher capacity than conventional relays. The schemes inspired by the aligned interference neutralization mechanism in [8] were investigated there, with which relays receive desired and interference signals from source nodes and reconstruct them before forwarding them to the destinations so as to achieve partial elimination of interference (i.e., IN) at the destinations and preserve the desired signal. Achievable DoFs of the interference channel were derived in [11], whereas an achievable rate region and its boundary of an instantaneous interference relay channel were studied in [12].

Note, however, that none of the existing IM methods are cost-free. For example, by adjusting a transmit beam using ZFBF or IA, the strength of the adjusted signal is attenuated; a zero-forcing based filter can be adopted to nullify interference at a loss of the desired signal power; with IN, an interfering signal is duplicated to neutralize the interference at the cost of extra transmit power consumption. Moreover, ZFBF, ZF reception, and IA require more DoFs than IN, to distinguish the desired signal from interference. For ZFBF and ZF reception, the DoF requirement is determined by the total number of desired signals and interferences, i.e., each interfering signal component consumes one DoF, whereas for

IA at least one DoF should be provided to place the aligned interference. In addition, when multiple interferences are from one identical transmitter, IA is not applicable. If the interfering signals originated from the same source are aligned in one direction, they will also overlap with each other at their intended receiver, thus becoming indistinguishable. With IN, since interference(s) can be neutralized over the air, no extra DoF for interference is required, thus becoming free from the aforementioned limitations of ZFBF, ZF reception and IA.

TABLE I
COMPARISON OF IM METHODS.

Feature \ Method	ZFBF	ZF	IA	IN
Tx/Rx side processing	Tx	Rx	Tx	Tx
Tx beam is adjusted	○	×	○	×
Rx beam is adjusted	×	○	×	×
Effective signal power loss	○	○	○	×
Tx power cost	×	×	×	○
Tx side CSI exchange	○	×	○	○
Tx side data exchange	×	×	×	○
Rx side full CSI	×	○	×	×
DoF cost w.r.t. interference	○	○	○	×
Symbol-level synchrony	×	×	×	○

Table I compares ZFBF, ZF, IA and IN, where the symbols ○ and × indicate having and not having the corresponding feature, respectively. Tx (Transmitter) beam indicates data transmission from various transmitters except for the sending of duplicated neutralizing signal. Rx (Receiver) beam means the direction of the receive filter's main lobe. Either Tx or Rx beam adjustment will cause effective signal power loss. Rx side full CSI (Channel state information) indicates the receiver needs to acquire CSI from all Txs, including intended and unintended Txs, to it. Although IN requires both CSI and data exchanges at the Tx side, as well as symbol-synchrony, since it has an advantage in saving DoFs over the other schemes, we will in this paper focus on the adaptive IM design based on dynamic and intelligent application of IN.

As discussed above, desired signal power loss and DoF cost are two major overheads in the design of IM mechanisms. However, existing IM methods focus only on the suppression, elimination or adjustment of interference without considering their overheads. We should not use an IM method if its performance loss outweighs its benefit. Due to the randomness of network topology and wireless channels, as well as transmit power differences of various communication equipments, the relationship of desired and interference signals, the tradeoff between the benefit of IM and the attenuation of the intended signal's power change dynamically. We must therefore investigate the problem of adaptively selecting IM methods and their operating parameters under various communication scenarios to achieve good transmission performance. Moreover, as for IN, the existing studies simply assume complete neutralization of interference without considering its power cost. The more transmit power is spent on interference neutralization, the less power for the desired signal's transmission will be available. Then, one can easily raise a question: "is complete IN always necessary?" In this paper, we will first propose *dynamic IN* (DIN) to address how much interference should be neutralized so that the users' spectral efficiency can be maximized. Then, adaptive selection between DIN and other IM methods will be presented to improve users' SE further in dynamically changing network environments.

The contributions of this paper are two-fold:

- Proposal of a novel IM scheme called *dynamic interference neutralization* (DIN). By intelligently determining the appropriate portion of interference to be neutralized, we balance the transmitter power used for IN and that for the desired signal's transmission. DIN can also subsume complete IN and non-IM as special cases, making it more general.
- Development of an adaptive IM mechanism incorporating DIN and some other IM methods. A proper IM method is selected by taking into account both its benefits and cost, thus improving the users' SE.

The rest of this paper is organized as follows. Section II describes the system model, while Section III details the DIN. Section IV presents the adaptive selection of IM schemes and Section V evaluates its performance and overhead. Finally, Section VI concludes the paper.

Throughout this paper, we use the following notations. The set of complex numbers is denoted as $\mathbb{C}$, while vectors and matrices are represented by bold lower-case and upper-case letters, respectively. Let $\mathbf{X}^H$ and $\mathbf{X}^{-1}$ denote the Hermitian and inverse of matrix $\mathbf{X}$. $\|\cdot\|$ and $|\cdot|$ indicate the Euclidean norm and the absolute value. $\mathbb{E}(\cdot)$ denotes statistical expectation and $\langle \mathbf{a}, \mathbf{b} \rangle$ represents the inner product of two vectors.

II. SYSTEM MODEL

We consider the downlink transmission in heterogeneous cellular networks composed of overlapping macro and pico cells [13]. As shown in Fig. 1, macro and pico base stations (MBS and PBS) are equipped with N_{T_1} and N_{T_0} antennas, whereas macro user equipment (MUE) and pico user equipment (PUE) have N_{R_1} and N_{R_0} antennas, respectively. Since mobile stations/devices are subject to severer restrictions in cost and hardware, than a base station (BS), the number of BS's antennas is assumed to be equal to or greater than the number of UE's antennas, i.e., $N_{T_i} \geq N_{R_i}$ where $i = 0, 1$. We also assume beamforming (BF) is adopted, and MBS and PBS send single data streams, x_1 and x_0, to MUE and PUE, respectively. $\mathbb{E}(\|x_1\|^2) = \mathbb{E}(\|x_0\|^2) = 1$ holds. The radio range, d, of a picocell is known to be $300m$ or less, whereas the radius, D, of a macrocell is taken $3000m$ [13]. Let P_{T_1} and P_{T_0} be the transmit power of MBS and PBS, respectively.

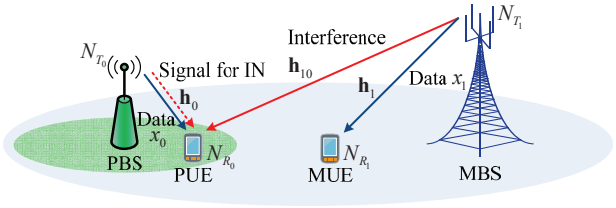

Fig. 1. System model.

The picocell operates in an open mode and allows the users within its coverage to access it. The transmission from MBS to

MUE will interfere with the intended transmission from PBS at PUE. Nevertheless, due to the limited coverage of a picocell, PBS will not cause too much interference to MUE, thus is omitted in our study. Let $\mathbf{h}_0 \in \mathbb{C}^{N_{R_0} \times N_{T_0}}$, $\mathbf{h}_1 \in \mathbb{C}^{N_{R_1} \times N_{T_1}}$ and $\mathbf{h}_{10} \in \mathbb{C}^{N_{R_0} \times N_{T_1}}$ represent the channel status from PBS to PUE, from MBS to MUE, and from MBS to PUE, respectively. A spatially uncorrelated Rayleigh flat fading channel model is used to model the elements of the above matrices as independent and identically distributed zero-mean unit-variance complex Gaussian random variables. We assume that all users experience block fading, i.e., channel parameters remain constant in a block consisting of several successive time slots and vary randomly between successive blocks. Each user can accurately estimate CSI w.r.t. its intended and unintended Txs and feed it back to the associated base station via a low-rate error-free link. We assume reliable links for the delivery of CSI and signaling. The delivery delay is negligible relative to the time scale on which the channel state varies.

Since picocells are deployed to improve the capacity and coverage of existing cellular systems, each picocell has subordinate features as compared to the macrocell, and hence the macrocell transmission is given priority over the picocell's transmission. However, we assume that PBS can acquire the information of x_1 via inter-BS collaboration; this is easy to achieve because PBS and MBS are deployed by the same operator [13]. With the above information, IN can be implemented to partially or completely neutralize the disturbance at PUE. Since the transmission from MBS to MUE depends only on $\mathbf{h}_1$ and is free from interference, we only focus on the pico-users' transmission performance.

III. Dynamic Interference Neutralization

As mentioned earlier, IN has recently received considerable attention, but existing studies simply assume the complete neutralization of interference without considering the tradeoff between the benefit of IN and its power cost. To remedy this deficiency, we propose a novel IM scheme called *dynamic interference neutralization* (DIN). By intelligently determining the appropriate portion of interference to be neutralized, DIN balances the transmitter power used for IN and that for the desired signal's transmission. Since the macrocell receives higher priority than picocells, MBS will not adjust its transmission for pico-users. Therefore, DIN is implemented by the PBS.

In the following discussion we use $N_{T_i} = N_{R_i} \geq 2$ where $i = 0, 1$ as an example, but our strategy can be easily extended to the case of $N_{T_i} \geq N_{R_i}$. Due to path loss, the received signal at PUE is expressed as:

$$\mathbf{y}_0 = \sqrt{P^e_{T_0}}\mathbf{h}_0\mathbf{p}_0x_0 + \sqrt{P^e_{T_1}}\mathbf{h}_{10}\mathbf{p}_1x_1 + \mathbf{z}_0 \tag{1}$$

where the column vectors $\mathbf{p}_0$ and $\mathbf{p}_1$ are the precoders for data symbols x_0 and x_1 at PBS and MBS, respectively. The first term on the right hand side (RHS) of Eq. (1) is the desired signal, the second term denotes the interference from MBS, and $\mathbf{z}_0$ is an additive white Gaussian noise (AWGN) vector whose elements have zero-mean and variance σ_n^2. For clarity of presentation, we define $P^e_{T_0} = P_{T_0}10^{-0.1L_0}$ and $P^e_{T_1} = P_{T_1}10^{-0.1L_{10}}$, where $P^e_{T_0}$ and $P^e_{T_1}$ indicate the transmit power of PBS and MBS with consideration of the path loss perceived by PUE. The path loss from MBS and PBS to a PUE is modeled as $L_{10} = 128.1 + 37.6log_{10}(\rho_{10}/10^3)\ dB$ and $L_0 = 38 + 30log_{10}(\rho_0)\ dB$, respectively [14], where the variable $\rho_{(\cdot)}$, measured in meters (m), is the distance from the transmitter to the receiver. With this definition, the consideration of various network topology and transmit power differences of various equipments can be simplified to $P^e_{T_0}$ and $P^e_{T_1}$.

The estimated signal at PUE after post-processing is

$$\bar{y}_0 = \mathbf{w}_0^H\mathbf{y}_0 \tag{2}$$

where $\mathbf{w}_0$ denotes the receive filter. Note that the interference model shown in Fig. 1 has an asymmetric feature in which only the interference from MBS to PUE is considered. Since the macrocell is given priority over the picocells, MBS will transmit messages to MUE based only on $\mathbf{h}_1$. Here we assume data transmissions based on the singular value decomposition (SVD), but can also use various types of pre- and post-processing method. Applying SVD to $\mathbf{h}_1$, we get $\mathbf{h}_1 = \mathbf{U}_1\mathbf{\Lambda}_1\mathbf{V}_1^H$. Then, we employ $\mathbf{p}_1 = \mathbf{v}_1^{(1)}$ and $\mathbf{w}_1 = \mathbf{u}_1^{(1)}$, where $\mathbf{w}_1$ represents the receive filter for x_1 at MUE. $\mathbf{v}_1^{(1)}$ and $\mathbf{u}_1^{(1)}$ are the first column vectors of the right and left singular matrices ($\mathbf{V}_1$ and $\mathbf{U}_1$), respectively, both of which correspond to the principal eigen-mode of $\mathbf{h}_1$.

With IN, PBS acquires interference information, including data and CSI, from MBS via inter-BS collaboration and by PUE's estimation and feedback, respectively. PBS then generates a duplicate of the interference and sends it along with the desired signal. The former is used for interference neutralization at PUE, whereas the latter carries the payload. The received signal at PUE then becomes:

$$\begin{aligned}\mathbf{y}_0 = &\sqrt{P^e_{T_0} - P^e_{IN}}\mathbf{h}_0\mathbf{p}_0x_0 + \sqrt{P^e_{T_1}}\mathbf{h}_{10}\mathbf{p}_1x_1 \\ &+ \sqrt{P^e_{IN}}\mathbf{h}_0\mathbf{p}_{IN}x_1 + \mathbf{z}_0\end{aligned} \tag{3}$$

where $P^e_{IN} = P_{IN}10^{-0.1L_0}$, P_{IN} represents the power overhead of IN, and $\mathbf{p}_{IN}$ is the precoder for the neutralizing signal. According to the complete IN [6–12], the interference terms in Eq. (3), $\sqrt{P^e_{T_1}}\mathbf{h}_{10}\mathbf{p}_1x_1$ and $\sqrt{P^e_{IN}}\mathbf{h}_0\mathbf{p}_{IN}x_1$, are fully neutralized with each other.

Since the use of IN doesn't require the adjustment of the intended signal's beam, in order to achieve as good transmission of x_0 as possible, the desired signal's delivery should be in line with its channel conditions. We apply SVD to $\mathbf{h}_0$ to obtain $\mathbf{h}_0 = \mathbf{U}_0\mathbf{\Lambda}_0\mathbf{V}_0^H$, and then adopt $\mathbf{p}_0 = \mathbf{v}_0^{(1)}$ and $\mathbf{w}_0 = \mathbf{u}_0^{(1)}$. $\mathbf{v}_0^{(1)}$ and $\mathbf{u}_0^{(1)}$ are the first column vectors of $\mathbf{U}_0$ and $\mathbf{V}_0$, respectively. To implement IN, the duplicated neutralizing signal should satisfy $\sqrt{P^e_{IN}}\mathbf{h}_0\mathbf{p}_{IN} = -\sqrt{P^e_{T_1}}\mathbf{h}_{10}\mathbf{p}_1$. The above equation can be decomposed into two parts, $\mathbf{h}_0\mathbf{p}_{IN} = -\mathbf{h}_{10}\mathbf{p}_1$ and $P^e_{IN} = P^e_{T_1}$ or equivalently $P_{IN} = P_{T_1}10^{0.1(L_0 - L_{10})}$. From $\mathbf{h}_0\mathbf{p}_{IN} = -\mathbf{h}_{10}\mathbf{p}_1$, we can get $\mathbf{p}_{IN} = -\mathbf{h}_0^{-1}\mathbf{h}_{10}\mathbf{p}_1$. Note that $\|\mathbf{p}_{IN}\| = 1$ is not guaranteed, i.e., $\mathbf{p}_{IN}$ has impact on the power cost of IN.

When $N_{T_i} > N_{R_i}$ $(i = 0, 1)$, the inverse of $\mathbf{h}_0$ should be replaced by its Moore-Penrose pseudo-inverse. The mechanism can then be generalized. Note that when the interference is too strong, P_{T_0} may not be sufficient for IN. In such a case, we simply switch to the non-IM mode. The achievable SE of PUE with complete IN is

$$r_0^{IN} = log_2\left\{1 + \frac{(P_{T_0} - P_{IN})10^{-0.1L_0}[\lambda_0^{(1)}]^2}{\sigma_n^2}\right\}, \quad (4)$$

where $\lambda_0^{(1)}$ is the largest singular value of $\mathbf{h}_0$ indicating the amplitude gain of the principal spatial sub-channel.

From Eq. (4) we can see that although the interference term is completely mitigated, it accompanies a transmit power loss, P_{IN}, degrading the received desired signal strength. One can then raise a question: "is complete IN always necessary/worthwhile?" To answer this question, we generalize the complete IN to *dynamic IN* by introducing a coefficient $\mu \in (0, 1]$ that indicates the portion of interference to be neutralized. When $\mu = 1$, the interference is fully neutralized, while DIN approaches non-IM as $\mu \to 0$. Similarly to the discussion about IN, to implement DIN, Eq. (5) should hold:

$$\sqrt{P_{DIN}^e}\mathbf{h}_0\mathbf{p}_{DIN} = -\sqrt{\mu P_{T_1}^e}\mathbf{h}_{10}\mathbf{p}_1 \quad (5)$$

where $P_{DIN}^e = P_{DIN}10^{-0.1L_0}$, P_{DIN} represents for the power consumption of DIN, and $10^{-0.1L_0}$ is the path loss from PBS to PUE. By defining the ratio of the path loss from MBS to PUE (i.e., $10^{-0.1L_{10}}$) to $10^{-0.1L_0}$ as $\varepsilon = 10^{0.1(L_0 - L_{10})}$, we get

$$\begin{cases} P_{DIN} = \mu\varepsilon P_{T_1}\|\mathbf{h}_0^{-1}\mathbf{h}_{10}\mathbf{p}_1\|^2 \\ \mathbf{p}_{DIN} = -\mathbf{h}_0^{-1}\mathbf{h}_{10}\mathbf{p}_1/\|\mathbf{h}_0^{-1}\mathbf{h}_{10}\mathbf{p}_1\| \end{cases}. \quad (6)$$

For clarity of exposition, we normalize the precoder so that the direction and strength requirements for DIN could be decoupled from each other, as given by Eq. (6). The achievable SE of PUE employing DIN can then be written as:

$$r_0^{DIN} = log_2\left\{1 + \frac{(P_{T_0} - P_{DIN})10^{-0.1L_0}[\lambda_0^{(1)}]^2}{\sigma_n^2 + I_r^{DIN}}\right\}, \quad (7)$$

where I_r^{DIN}, given by Eq. (8) below, denotes the residual interference, in which $\chi = [\mathbf{u}_0^{(1)}]^H\mathbf{h}_{10}\mathbf{p}_1$. We further define $\mathbf{g} = \mathbf{h}_0^{-1}\mathbf{h}_{10}\mathbf{p}_1$, which can be regarded as the precoder for IN without normalization. Then, the signal-to-interference-plus-noise ratio (SINR) in Eq. (7) can be simplified as

$$\psi_{DIN} = \frac{(P_{T_0}^e - \mu P_{T_1}^e\|\mathbf{g}\|^2)[\lambda_0^{(1)}]^2}{\sigma_n^2 + P_{T_1}^e(1-\sqrt{\mu})^2|\chi|^2} = \frac{A - \mu B}{C - D\sqrt{\mu} + \mu E}, \quad (9)$$

$$\begin{aligned} I_r^{DIN} &= \left\{[\mathbf{u}_0^{(1)}]^H(\sqrt{P_{DIN}^e}\mathbf{h}_0\mathbf{p}_{DIN} + \sqrt{P_{T_1}^e}\mathbf{h}_{10}\mathbf{p}_1)\right\}\left\{[\mathbf{u}_0^{(1)}]^H(\sqrt{P_{DIN}^e}\mathbf{h}_0\mathbf{p}_{DIN} + \sqrt{P_{T_1}^e}\mathbf{h}_{10}\mathbf{p}_1)\right\}^H \\ &= \left(\sqrt{P_{T_1}^e} - \sqrt{\mu P_{T_1}^e}\right)^2\left\{[\mathbf{u}_0^{(1)}]^H\mathbf{h}_{10}\mathbf{p}_1\right\}\left\{[\mathbf{u}_0^{(1)}]^H\mathbf{h}_{10}\mathbf{p}_1\right\}^H = P_{T_1}^e(1-\sqrt{\mu})^2|\chi|^2 \end{aligned} \quad (8)$$

$$\begin{aligned} BC + AE - \sqrt{AB}D &= P_{T_1}^e\|\mathbf{g}\|^2[\lambda_0^{(1)}]^2(\sigma_0^2 + P_{T_1}^e|\chi|^2) + P_{T_0}^e[\lambda_0^{(1)}]^2P_{T_1}^e|\chi|^2 - 2\sqrt{P_{T_0}^e[\lambda_0^{(1)}]^2P_{T_1}^e\|\mathbf{g}\|^2[\lambda_0^{(1)}]^2}P_{T_1}^e|\chi|^2 \\ &> (P_{T_1}^e)^2\|\mathbf{g}\|^2[\lambda_0^{(1)}]^2|\chi|^2 + P_{T_0}^eP_{T_1}^e[\lambda_0^{(1)}]^2|\chi|^2 - 2(P_{T_0}^e)^{\frac{1}{2}}(P_{T_1}^e)^{\frac{3}{2}}[\lambda_0^{(1)}]^2\|\mathbf{g}\||\chi|^2 \\ &= P_{T_1}^e[\lambda_0^{(1)}]^2|\chi|^2\left[(P_{T_1}^e)^{\frac{1}{2}}\|\mathbf{g}\| - (P_{T_0}^e)^{\frac{1}{2}}\right]^2 \geq 0 \end{aligned}. \quad (13)$$

where $A = P_{T_0}^e[\lambda_0^{(1)}]^2$, $B = P_{T_1}^e\|\mathbf{g}\|^2[\lambda_0^{(1)}]^2$, $C = \sigma_n^2 + P_{T_1}^e|\chi|^2$, $D = 2P_{T_1}^e|\chi|^2$ and $E = P_{T_1}^e|\chi|^2$. Note that all of these coefficients are positive.

In what follows, we will discuss the existence of optimal μ, denoted by $\mu^* \in (0, \mu_{max}]$, with which ψ_{DIN} is maximized under the P_{T_0} constraint. $\mu_{max} = min\left(1, \frac{P_{T_0}^e}{P_{T_1}^e\|\mathbf{g}\|^2}\right)$. If $P_{T_0}^e > P_{T_1}^e\|\mathbf{g}\|^2$, PBS has enough power to completely neutralize the interference. Otherwise, when $P_{T_0}^e < P_{T_1}^e\|\mathbf{g}\|^2$, μ_{max} is limited by the transmit power at PBS. In what follows, We first prove the solvability of μ^*, and then show the quality of the solution(s).

By computing the derivative of ψ_{DIN} to μ and setting it to 0, we have

$$\frac{-B(C - D\sqrt{\mu} + \mu E) - (A - \mu B)(E - \frac{D}{2\sqrt{\mu}})}{(C - D\sqrt{\mu} + \mu E)^2} = 0. \quad (10)$$

Since the denominator cannot be 0, we only need to solve

$$-B(C - D\sqrt{\mu} + \mu E) - (A - \mu B)\left(E - \frac{D}{2\sqrt{\mu}}\right) = 0. \quad (11)$$

By simplifying (11), a quadratic equation with one unknown is obtained as:

$$\frac{BD}{2}\xi^2 - (BC + AE)\xi + \frac{AD}{2} = 0, \quad (12)$$

where $\xi = \sqrt{\mu} > 0$. Let $\Delta = (BC + AE)^2 - ABD^2$; if $\Delta \geq 0$ holds, then ξ is solvable. Since $\Delta = (BC + AE + \sqrt{AB}D)(BC + AE - \sqrt{AB}D)$, and $BC + AE + \sqrt{AB}D$ is positive, we only need to show that $BC + AE - \sqrt{AB}D > 0$. The proof is given by Eq. (13) below.

Based on the above discussion, solutions $\xi_\pm^* = \frac{(BC+AE)\pm\sqrt{\Delta}}{BD}$ are obtained. (Note that $\xi_\pm^* \in (0, \sqrt{\mu_{max}}]$ should hold.) We then need to verify the qualification of the two solutions. We first investigate the feasibility of the larger solution $\xi_+^* = \frac{(BC+AE)+\sqrt{\Delta}}{BD}$. The first term of ξ_+^* can be rewritten as

$$\begin{aligned} \frac{BC + AE}{BD} &> \frac{P_{T_1}^e\|\mathbf{g}\|^2[\lambda_0^{(1)}]^2P_{T_1}^e|\chi|^2 + P_{T_0}^e[\lambda_0^{(1)}]^2P_{T_1}^e|\chi|^2}{2P_{T_1}^e\|\mathbf{g}\|^2[\lambda_0^{(1)}]^2P_{T_1}^e|\chi|^2} \\ &= \frac{1}{2} + \frac{P_{T_0}^e}{2P_{T_1}^e\|\mathbf{g}\|^2} \end{aligned}. \quad (14)$$

The second term of ξ_+^* is

$$\begin{aligned} \frac{\sqrt{\Delta}}{BD} &> \sqrt{\left(\frac{1}{2} + \frac{P_{T_0}^e}{2P_{T_1}^e\|\mathbf{g}\|^2}\right)^2 - \frac{P_{T_0}^e}{P_{T_1}^e\|\mathbf{g}\|^2}} \\ &= \left|\frac{1}{2} - \frac{P_{T_0}^e}{2P_{T_1}^e\|\mathbf{g}\|^2}\right| \end{aligned}. \quad (15)$$

Then, we can get

$$\xi_+^* > \left(\frac{1}{2} + \frac{P_{T_0}^e}{2P_{T_1}^e\|\mathbf{g}\|^2}\right) + \left|\frac{1}{2} - \frac{P_{T_0}^e}{2P_{T_1}^e\|\mathbf{g}\|^2}\right| = \begin{cases} 1, & \frac{P_{T_0}^e}{2P_{T_1}^e\|\mathbf{g}\|^2} \le \frac{1}{2} \\ \frac{P_{T_0}^e}{P_{T_1}^e\|\mathbf{g}\|^2}, & \frac{P_{T_0}^e}{2P_{T_1}^e\|\mathbf{g}\|^2} > \frac{1}{2}. \end{cases} . \quad (16)$$

Note that $\xi_+^* \le 1$, and hence $\frac{P_{T_0}^e}{2P_{T_1}^e\|\mathbf{g}\|^2}$ should not be less than or equal to $\frac{1}{2}$. However, when $\frac{P_{T_0}^e}{2P_{T_1}^e\|\mathbf{g}\|^2} > \frac{1}{2}$, $\xi_+^* > \frac{P_{T_0}^e}{P_{T_1}^e\|\mathbf{g}\|^2}$ is equivalent to $\xi_+^* > 1$. As a result, $\xi_+^* \notin (0, \sqrt{\mu_{max}}]$, where $\mu_{max} = min\left(1, \frac{P_{T_0}^e}{P_{T_1}^e\|\mathbf{g}\|^2}\right)$, i.e., ξ_+^* is not acceptable.

As for $\xi_-^* = \frac{(BC+AE)-\sqrt{\Delta}}{BD}$, since $ABD^2 > 0$, $BC + AE > \sqrt{\Delta}$ holds, thus justifying $\xi_-^* > 0$. We prove $\xi_-^* \le \sqrt{\mu_{max}}$ as follows. First, we define a function $f(C) = (BC + AE) - \sqrt{\Delta}$. Since the derivative of $f(C)$ to C, $f'(C) = \frac{B\sqrt{\Delta} - B(BC+AE)}{\sqrt{\Delta}} < 0$, $f(C)$ is a monotonically decreasing function of variable C. Let $C' = P_{T_1}^e|\chi|^2$, then $C = \sigma_n^2 + P_{T_1}^e|\chi|^2 > C'$, thus leading to $f(C) < f(C')$. Similarly to the derivations of Eqs. (14)–(16), we get

$$\xi_-^* = \frac{f(C)}{BD} < \frac{f(C')}{BD} = \begin{cases} 1, & \frac{P_{T_0}^e}{2P_{T_1}^e\|\mathbf{g}\|^2} \ge \frac{1}{2} \\ \frac{P_{T_0}^e}{P_{T_1}^e\|\mathbf{g}\|^2}, & \frac{P_{T_0}^e}{2P_{T_1}^e\|\mathbf{g}\|^2} < \frac{1}{2} \end{cases} . \quad (17)$$

Eq. (17) is equivalent to $\xi_-^* < \mu_{max} = min(1, \frac{P_{T_0}^e}{P_{T_1}^e\|\mathbf{g}\|^2})$. Also, since $0 < \mu_{max} \le 1$, $\mu_{max} \le \sqrt{\mu_{max}}$ holds, thus proving $\xi_-^* < \sqrt{\mu_{max}}$.

In the end, we prove that ξ_-^* could achieve the maximum ψ_{DIN}. Since it can be proved that $g(\xi) = \frac{BD}{2}\xi^2 - (BC + AE)\xi + \frac{AD}{2}$ is a monotonically decreasing function of variable $\xi \in (0, \sqrt{\mu_{max}}]$, when $0 < \xi < \xi_-^*$, we get $g(\xi) > \frac{BD}{2}(\xi_-^*)^2 - (BC + AE)\xi_-^* + \frac{AD}{2} = 0$. Similarly, when $\xi_-^* < \xi < \sqrt{\mu_{max}}$, $g(\xi) < 0$ can be derived. Thus, ξ_-^* corresponds to the maximum ψ_{DIN}. When DIN is employed, an optimal portion of interference should therefore be neutralized to achieve the maximum PUE's SE. The optimal neutralization coefficient is calculated as $\mu^* = (\xi_-^*)^2$.

IV. Adaptive Selection of IM Methods

So far, we have proved that an appropriate portion of interference needs to be neutralized so as to balance the transmitter's power used for IN and that for the desired signal's transmission. However, DIN is not free, although it is an optimal design compared to complete IN. Thus, we need to address how to intelligently select IM methods by taking into account their benefits and cost under various communication situations.

Since the macrocell is given priority over picocells, MBS will not adjust its transmission for pico-users. IM should thus be implemented at PBS or/and PUE. According to Eq. (2), there are different ways of designing $\mathbf{p}_0$ and $\mathbf{w}_0$ to achieve IM. In what follows, we study the adaptation of four typical IM methods — non-IM (mode I), ZF reception at PUE (mode II), ZFBF at PBS combined with the matched filter (MF) at PUE (mode III), and DIN — to improve the pico-users' SE. In case of mode III, we use the concept of ZFBF but modify the implementation, i.e., we let the transmitter corresponding to the victim receiver adjust its beam so that the desired signal is orthogonal to the interference at the intended receiver. Note, however, that other IM schemes than those mentioned above can also be included in the following discussion.

We first present a general expression of SINR at a receiver which or/and the intended transmitter of which performs IM, as given in Eq. (18); from this one can easily see the tradeoff between the benefits and cost of IM.

$$\psi_{\mathcal{M}} = \frac{\left[P_{T_0} - P_{\mathcal{M}}^{OH}\right] 10^{-0.1L_0} \left\|(\mathbf{w}_0^{\mathcal{M}})^H \mathbf{h}_0 \mathbf{p}_0^{\mathcal{M}}\right\|^2}{\sigma_n^2 + I_r^{\mathcal{M}}} \quad (18)$$

where the superscript or subscript $\mathcal{M}$ denotes the index of IM mode. $P_{\mathcal{M}}^{OH}$ represents for the power cost at Tx with IM mode $\mathcal{M}$. $\mathbf{p}_0$ and $\mathbf{w}_0$ are the precoder and the receive filter employed for the desired transmission, while $\mathbf{p}_1$ indicates the precoder at the interfering Tx. When $\mathcal{M} \in \{I,\ II,\ III\}$, $P_{\mathcal{M}}^{OH} = 0$ and $I_r^{\mathcal{M}} = P_{T_1} 10^{-0.1L_{10}} \left\|(\mathbf{w}_0^{\mathcal{M}})^H \mathbf{h}_{10}\mathbf{p}_1\right\|^2$, whereas for DIN, I_r^{DIN} is calculated using Eq. (8). $\left\|(\mathbf{w}_0^{\mathcal{M}})^H \mathbf{h}_0 \mathbf{p}_0^{\mathcal{M}}\right\|^2$ and $I_r^{\mathcal{M}}$ reflect the attenuation of the intended signal's power and the extent of interference mitigation, respectively. As can be seen from Eq. (18), reducing the interference term in the denominator of $\psi_{\mathcal{M}}$ incurs a loss of the desired signal power, indicated by the numerator of $\psi_{\mathcal{M}}$. In what follows, we use SVD-based pre- and post-processing as an example, but can in practice use any processing method. Note that when $I_r^{\mathcal{M}} = 0$, SINR becomes SNR.

When non-IM is employed by a picocell, we simply use $\mathbf{p}_0^I = \mathbf{v}_0^{(1)}$ and $\mathbf{w}_0^I = \mathbf{u}_0^{(1)}$. In this case, $P_I^{OH} = 0$, so we have the SINR at PUE as:

$$\psi_I = \frac{P_{T_0}^e [\lambda_0^{(1)}]^2}{\sigma_n^2 + P_{T_1}^e \left\|(\mathbf{w}_0^I)^H \mathbf{h}_{10}\mathbf{p}_1\right\|^2}. \quad (19)$$

The PUE's achievable SE can be calculated using Shannon's Theorem.

With ZF reception (mode II), PUE designs $\mathbf{w}_0^{II}$ to nullify the MBS's interference. We employ $\mathbf{p}_1 = \mathbf{v}_1^{(1)}$, $\mathbf{w}_1 = \mathbf{u}_1^{(1)}$ and $\mathbf{p}_0^{II} = \mathbf{v}_0^{(1)}$, and leave $\mathbf{w}_0^{II}$ to be calculated. $\mathbf{w}_0^{II}$ should be orthogonal to $\mathbf{h}_{10}\mathbf{p}_1$ so that the interference term after filtering, $\sqrt{P_{T_1}^e}(\mathbf{w}_0^{II})^H \mathbf{h}_{10}\mathbf{p}_1 x_1$, becomes 0. We first project $\mathbf{u}_0^{(1)}$ onto the orthogonal direction of $\mathbf{h}_{10}\mathbf{p}_1$. Then, the result is normalized to obtain $\mathbf{w}_0^{II}$. Let $\mathbf{v}_\pi = \mathbf{h}_{10}\mathbf{p}_1 / \|\mathbf{h}_{10}\mathbf{p}_1\|$, then $\mathbf{w}_0^{II} = \frac{\mathbf{u}_0^{(1)} - \mathbf{v}_\pi^H \mathbf{u}_0^{(1)} \mathbf{v}_\pi}{\|\mathbf{u}_0^{(1)} - \mathbf{v}_\pi^H \mathbf{u}_0^{(1)} \mathbf{v}_\pi\|}$. SNR at the PUE is

$$\psi_{II} = P_{T_0}^e \left\|(\mathbf{w}_0^{II})^H \mathbf{h}_0 \mathbf{p}_0^{II}\right\|^2 / \sigma_n^2. \quad (20)$$

Eq. (20) can be simplified further as:

$$\psi_{II} = P_{T_0}^e [\lambda_0^{(1)}]^2 \left|\langle \mathbf{w}_0^{II}, \mathbf{u}_0^{(1)} \rangle\right|^2 / \sigma_n^2. \quad (21)$$

Since $\left|\langle \mathbf{w}_0^{II}, \mathbf{u}_0^{(1)} \rangle\right| < 1$, some power loss of the desired signal is accompanied.

Besides non-IM (mode I) and IM processing at the victim receiver end (i.e., ZF reception (mode II)), IM can also be

implemented at the transmitter. With mode III, PBS adjusts its transmit beam so that the spatial feature of the desired signal, $\mathbf{h}_0\mathbf{p}_0$, may be orthogonal to that of the interference from MBS, $\mathbf{h}_{10}\mathbf{p}_1$, observed at PUE. Then, PUE applies MF to recover x_0.

We first design $\mathbf{p}_0^{III}$ to make $\mathbf{h}_0\mathbf{p}_0^{III}$ orthogonal to $\mathbf{h}_{10}\mathbf{p}_1$. Then, we determine $\mathbf{w}_0^{III}$ matched with the desired signal's signature $\mathbf{h}_0\mathbf{p}_0^{III}$. Let $\mathbf{v}_\pi = \mathbf{h}_{10}\mathbf{p}_1/\|\mathbf{h}_{10}\mathbf{p}_1\|$, a unit vector $\mathbf{v}_\perp = \frac{\mathbf{v}_0^{(1)} - \mathbf{v}_\pi^H\mathbf{v}_0^{(1)}\mathbf{v}_\pi}{\|\mathbf{v}_0^{(1)} - \mathbf{v}_\pi^H\mathbf{v}_0^{(1)}\mathbf{v}_\pi\|}$ which is orthogonal to $\mathbf{h}_{10}\mathbf{p}_1$, or equivalently $\mathbf{v}_\pi$, can be found. Then, $\mathbf{p}_0^{III} = \mathbf{h}_0^{-1}\mathbf{v}_\perp/\|\mathbf{h}_0^{-1}\mathbf{v}_\perp\|$ and $\mathbf{w}_0^{III} = \mathbf{h}_0\mathbf{p}_0^{III}/\|\mathbf{h}_0\mathbf{p}_0^{III}\|$. The achievable SINR of PUE can be calculated in terms of Eq. (20) by replacing $\mathbf{p}_0^{II}$ and $\mathbf{w}_0^{II}$ with $\mathbf{p}_0^{III}$ and $\mathbf{w}_0^{III}$, respectively. Similarly to the analysis of mode II, as $\left|\langle \mathbf{w}_0^{III}, \mathbf{h}_0\mathbf{p}_0^{III}\rangle\right| < \lambda_0^{(1)}$, the loss of the desired signal power results, degrading the PUE's SNR as well as its achievable SE.

We present criteria aiming to achieve as high ψ and PUE's achievable SE as possible, with which different IM modes can be selected adaptively.

We first compare ψ_{DIN} with SINR/SNR of the other IM modes. Let $P_{T_0}^e = \eta P_{T_1}^e$, $\gamma = P_{T_1}^e/\sigma_n^2$ and $\varepsilon = 10^{0.1(L_0 - L_{10})}$. In case of DIN, we assume the optimal μ^* is employed. Note that $P_{DIN}10^{-0.1L_0} = \mu^* P_{T_1}^e\|\mathbf{g}\|^2$, as can be seen from Eqs. (7) and (9). By letting $\psi_I > \psi_{DIN}$, we have

$$\frac{1}{\sigma_n^2 + P_{T_1}^e\left\|(\mathbf{w}_0^I)^H\mathbf{h}_{10}\mathbf{p}_1\right\|^2} > \frac{1 - \frac{P_{DIN}^e}{P_{T_0}^e}}{\sigma_n^2 + I_r}. \tag{22}$$

By simplifying Eq. (22), we can obtain

$$\|\mathbf{g}\|^2 > \frac{P_{T_1}^e\|\alpha\|^2 - I_r}{\frac{\sigma_n^2}{\eta}\mu^* + \frac{P_{T_1}^e}{\eta}\mu^*\|\alpha\|^2} = \frac{\eta\gamma}{\mu^*}\frac{\|\alpha\|^2 - (1-\sqrt{\mu^*})^2|\chi|^2}{1 + \|\alpha\|^2\gamma} \tag{23}$$

where $\alpha = (\mathbf{w}_0^I)^H\mathbf{h}_{10}\mathbf{p}_1$. When Eq. (23) holds, non-IM is preferred to DIN.

Next, we compare ψ_{DIN} to ψ_{II} and ψ_{III}. Both ψ_{II} and ψ_{III} can be calculated by following Eq. (18). Recall that $P_{DIN}^e = P_{DIN}10^{-0.1L_0}$, $P_{T_1}^e = P_{T_1}10^{-0.1L_{10}}$, and $P_{DIN} = \mu\varepsilon P_{T_1}\|\mathbf{g}\|^2$. Let $\psi_{II/III} > \psi_{DIN}$, then similarly to the derivation of Eq. (23), we obtain

$$\|\mathbf{g}\|^2 > \frac{\eta}{\mu^*}\left\{1 - \frac{1 + \gamma(1-\sqrt{\mu^*})^2|\chi|^2}{[\lambda_0^{(1)}]^2}\|\beta^{II/III}\|^2\right\} \tag{24}$$

where $\beta^{II/III} = (\mathbf{w}_0^{II/III})^H\mathbf{h}_0\mathbf{p}_0$. When Eq. (24) holds, $\psi_{II/III}$ exceeds ψ_{DIN}. Note that if MBS could make an adjustment to avoid interference to PUE, $\mathbf{p}_0^{II/III} = \mathbf{v}_0^{(1)}$ and $\mathbf{w}_0^{II/III} = \mathbf{u}_0^{(1)}$ can be adopted by PBS and PUE, respectively. Then, we have $\beta^{II/III} = \lambda_0^{(1)}$ and $\|\mathbf{g}\|^2 > 0$ holds definitely, i.e., DIN is not necessary. In the above situation, neither mode II nor III is necessary, i.e., no need for IM in a picocell since MBS handles the interference to PUE.

We now compare ψ_I with ψ_{II} and ψ_{III}. By letting $\psi_I > \psi_{II/III}$, we get

$$\frac{[\lambda_0^{(1)}]^2}{1 + \gamma\|\alpha\|^2} > \|\beta^{II/III}\|^2 \tag{25}$$

Algorithm 1 Adaptive selection of IM methods

Initialization:
PBS acquires interference information and computes precoders and filters under different IM modes;

Procedure:
if Eq. (23) holds **then**
  if Eq. (25) holds (β^{II} is considered) **then**
    if Eq. (25) holds (β^{III} is considered) **then**
      Mode I is adopted;
    else
      Mode III is employed;
    end if
  else
    if Eq. (26) holds **then**
      Mode II is adopted;
    else
      Mode III is employed;
    end if
  end if
else
  if Eq. (24) holds (β^{II} is considered) **then**
    if Eq. (26) holds **then**
      Mode II is adopted;
    else
      Mode III is employed;
    end if
  else
    if Eq. (24) holds (β^{III} is considered) **then**
      Mode III is adopted;
    else
      DIN is employed;
    end if
  end if
end if

where $\alpha = (\mathbf{w}_0^I)^H\mathbf{h}_{10}\mathbf{p}_1$. When Eq. (25) holds, non-IM is adopted.

Finally, mode II and III are compared. When the following inequality holds, mode II is preferred.

$$[\lambda_0^{(1)}]^2\left|\langle \mathbf{w}_0^{II}, \mathbf{u}_0^{(1)}\rangle\right|^2 > \|\beta^{III}\|^2. \tag{26}$$

Algorithm 1 shows how to implement the adaptive selection of IM modes. Collaboration between picocells and a macrocell is required in practice so that PUE is able to estimate both $\mathbf{h}_0$ and $\mathbf{h}_{10}$ and feed back to PBS. In addition, an explicit or implicit low rate control channel should be employed [15] so that PBS could inform PUE of the IM mode being used.

So far, we have considered only one desired signal and interference in the design of DIN. When there are multiple interfering signals from a MBS, DIN can be applied to each of the interferences separately, or the constructive/destructive interactions among these interfering signals can be exploited to reduce the dimension of interference [16]. We can generate a signal for dynamic IN by exploiting the combined interference $\sum_{k=1}^K \sqrt{P_{T_{1,k}}^e}\mathbf{h}_{10}\mathbf{p}_{1,k}x_{1,k}$, where $\mathbf{x}_1 = [x_{1,1}, \cdots, x_{1,k}, \cdots, x_{1,K}]$ is the MBS's transmit data vector and $P_{T_{1,k}}^e$ is the Tx power for $x_{1,k}$, i.e., $P_{1,k}$, incorporated with the path loss $10^{-0.1L_{10}}$. In the case of multiple desired signals, DIN can be applied directly to mitigate the

interference regardless of the number of intended transmissions, i.e., DIN can be extended to the case of multiple desired signals.

V. Simulation Results

MATLAB simulation is used to evaluate the adaptive IM methods incorporated with DIN. We set $d = 300m$, $D = 3000m$, $P_{T_0} = 23dBm$ and $P_{T_1} = 46dBm$ [13, 17]. Path loss are set to $L_{10} = 128.1 + 37.6log_{10}(\rho_{10}/10^3)\ dB$ and $L_0 = 38+30log_{10}(\rho_0)\ dB$ as in [14] where $\rho_0 \leq d$ and $\rho_{10} \leq D$. Since L_0 and L_{10} are dependent on the network topology, $P^e_{T_0}$ ranges from $-89dBm$ to $23dBm$, whereas $P^e_{T_1}$ varies between $-100dBm$ to $46dBm$. For clarity of presentation, we adopt $\bar{\gamma} = 10lg(\gamma)$ where $\gamma = P^e_{T_1}/\sigma^2_n$. Recall that η is defined as $\eta = P^e_{T_0}/P^e_{T_1}$. Based on these parameter settings, $\eta \in [-135, 123]\ dB$. Note, however, that we obtained this result for extreme boundary situations, so its range is too wide to be useful. In practice, a PBS should not be deployed close to MBS and mobile users may select an access point based on the strength of reference signals from multiple access points. Based on this practice, we set $\eta \in [0.1, 100]$ in our simulation.

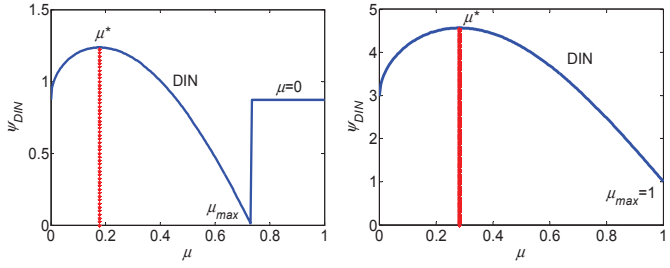

(a) Strong interference. (b) Weak interference.

Fig. 2. ψ_{DIN} vs. μ under $N_{T_0} = N_{R_0} = N_{T_1} = 2$, $\bar{\gamma} = 0dB$, and $\eta = 2$.

Fig. 2 shows two samples of the relationship between ψ_{DIN} and μ. The interference shown in Fig. 2(a) is relatively strong, and hence, when $\mu > \mu_{max}$ where $\mu_{max} < 1$, there won't be enough power for PBS to neutralize the interference. In such a case, we simply switch off IN and adopt non-IM (mode I) with which $\psi_I = \frac{P^e_{T_0}[\lambda^{(1)}_0]^2}{\sigma^2_n + P^e_{T_1}|\chi|^2}$. Non-IM can be included as a special case of DIN by setting $\mu = 0$. Since the interfering signal in Fig. 2(b) is weak, it can be completely neutralized, i.e., μ_{max} can be as large as 1. In both figures, the optimal μ, denoted by μ^*, is computed as in Section III, which corresponds to the maximum ψ_{DIN}. We can conclude from Fig. 2 that in order to better utilize the transmit power for both IN and data transmission, it is necessary to intelligently determine an appropriate portion of interference to be neutralized.

Fig. 3 plots the PUE's average SE versus μ for different η. As can be seen from the figure, the average μ^* grows as η increases. Since non-IM can be regarded as a special case of DIN, non-IM's SE cannot exceed DIN's. When η gets too high, a large portion of interference is preferred to be neutralized. As shown in the figure, provided that $\eta = 100$, the average μ^* is approximately 0.9. In addition, since the strength of the desired signal relative to the interference grows with an increase of η, the PUE's SE performance improves with η.

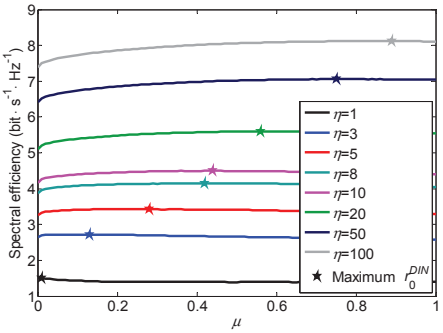

Fig. 3. Spectral efficiency of PUE vs. μ under $N_{T_0} = N_{R_0} = N_{T_1} = 2$, $\bar{\gamma} = 0dB$, and different η.

Fig. 4 shows the average μ^* under $N_{T_0} = N_{R_0} = N_{T_1} = 2$, different η and $\bar{\gamma}$. With fixed η, the average μ^* grows with an increase of $\bar{\gamma}$. This is because the interference gets stronger with $\bar{\gamma}$, and hence, to achieve the maximum SE, the optimal μ should increase with $\bar{\gamma}$, i.e., preferring more interference to be neutralized. With the same $\bar{\gamma}$, the average μ^* grows with an increase of η, which is consistent with Fig. 3.

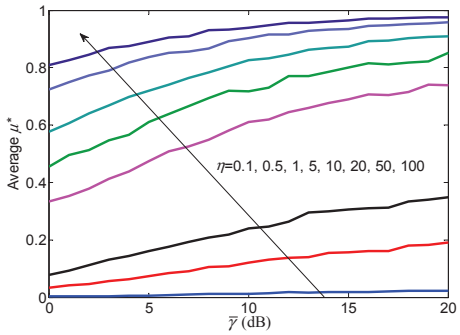

Fig. 4. Average μ^* vs. $\bar{\gamma}$ under $N_{T_0} = N_{R_0} = N_{T_1} = 2$ and different η.

Fig. 5 plots PUE's average SE along with μ under different antenna settings. We use a general form $[N_{T_0}\ N_{R_0}\ N_{T_1}]$ to express the antenna configuration. $N_{T_0} = N_{T_1}$ is fixed in Fig. 5(a). The average μ^*, marked by pentagram, decreases, while PUE's SE increases as N_{R_0} increases. With such antenna settings, since N_{T_0} and N_{T_1} are fixed, the processing gain with the transmit antenna array doesn't change for the desired signal or the interference. However, as N_{R_0} increases, the receive gain for intended signal grows as the filter vector $\mathbf{w}_0$ — designed to match $\mathbf{h}_0$ — is an $N_{R_0} \times 1$ vector. As a result, the desired signal, relative to the interference, after receive filtering becomes stronger with an increase of N_{R_0}, thus enhancing the PUE's SE and reducing the average μ^*. In Fig. 5(b), N_{R_0} and N_{T_1} are fixed, and N_{T_0} varies from 2 to 8. Since the transmit array gain of desired signal grows with an increase of N_{T_0}, and more interference can be neutralized with the same power overhead as N_{T_0} grows, both the average μ^* and the achievable SE improve as N_{T_0} increases. In Fig. 5(c), N_{T_0} and N_{R_0} are fixed while N_{T_1} ranges from 2 to 8. Although N_{T_1} varies, MBS causes random interferences to PUE as PUE adopts $\mathbf{w}_0$ to decode x_0 regardless of the interference channel $\mathbf{h}_{10}$. Hence, both μ^* and the PUE's average SE under different N_{T_1} remain similar.

Based on Figs. 3–5, the relationships of μ^* and PUE's

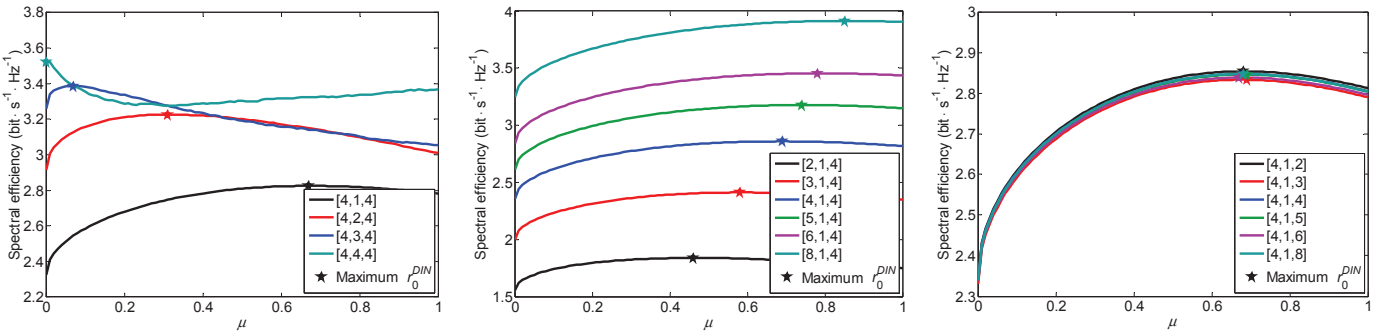

(a) N_{R_0} is variable. (b) N_{T_0} is variable. (c) N_{T_1} is variable.

Fig. 5. Spectral efficiency of PUE vs. μ under $\eta = 2$, $\bar{\gamma} = 0dB$, and different antenna settings.

SE with increases of parameters, η, $\bar{\gamma}$, N_{R_0}, N_{T_0} and N_{T_1} are summarized in Table II, where the symbols $\uparrow$, $\downarrow$ and – indicate increasing, decreasing, and invariable, respectively. Note, however, that the relation between PUE's SE and $\bar{\gamma}$ should be referred to Figs. 6 and 7.

TABLE II
THE RELATIONSHIPS OF μ^* AND PUE'S SE WITH INCREASES OF PARAMETERS.

Param.	η	$\bar{\gamma}$	N_{R_0}	N_{T_0}	N_{T_1}
μ^*	$\uparrow$	$\uparrow$	$\downarrow$	$\uparrow$	–
PUE's SE	$\uparrow$	$\uparrow$	$\uparrow$	$\uparrow$	–

Fig. 6 shows the PUE's achievable SE with different IM methods. r_0^{IN} is also plotted to demonstrate the advantage of DIN over complete IN. The upper bound of r_0 is obtained by adopting $\mathbf{p}_0 = \mathbf{v}_0^{(1)}$ and $\mathbf{w}_0 = \mathbf{u}_0^{(1)}$ without interference. Adaptive selection of IM is shown to provide the best SE among the fixed IM methods. In Fig. 6(a) with $\eta = 0.1$, the interference is relatively strong and the probability of P_{T_0} not being sufficient for complete IN is high. So, IN frequently switches to mode I, i.e., when complete IN is not available, non-IM is adopted. As for DIN, the optimal μ is close to 0 (non-IM) as shown in Figs. 3(a) and 5. Hence, r_0^{DIN} overlaps with r_0^I (non-IM) and r_0^{IN}. Modes II and III cause loss to the desired signal power while suppressing interference. Mode III causes more loss than mode II, resulting in inferior SE. When $\bar{\gamma}$ is low, noise is the dominant factor affecting the PUE's SE, the benefit of IM is limited, or even the cost of IM may outweigh its gain. As a result, r_0^I is close to, or even shows some advantage over r_0^{II}, r_0^{III}, r_0^{IN} and r_0^{DIN} at low $\bar{\gamma}$. When $\bar{\gamma}$ is large, the SE of modes II and III outperforms that of non-IM, or complete IN and DIN. Thus, it can be concluded that DIN is not suitable for managing relatively strong interference.

In Fig. 6(b), when η is large, $P_{T_0}^e$ is relatively stronger than the interfering signal that undergoes path loss. PBS is able to implement complete IN with a high probability. Non-IM is close to complete IN and DIN, and outperforms modes II and III at low $\bar{\gamma}$. The analysis is the same as that in Fig. 6(a). As $\bar{\gamma}$ increases, SE of modes II and III gradually exceeds that of non-IM, and the advantage of complete IN and DIN over non-IM becomes more pronounced.

Fig. 7 plots the achievable SE of PUE along with η for different IM schemes. In Fig. 7(a), when $\bar{\gamma}$ is small, the interference is weak relative to noise. Noise dominates the SE performance, and thus the contribution of IM to SE is

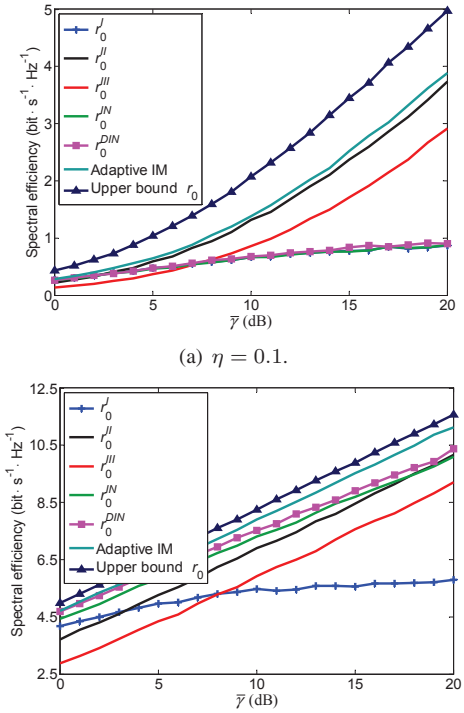

(a) $\eta = 0.1$.

(b) $\eta = 10$.

Fig. 6. Spectral efficiency of PUE vs. $\bar{\gamma}$ with various IM schemes under $N_{T_0} = N_{R_0} = N_{T_1} = 2$ and different η.

limited. Moreover, the desired signal's power loss caused by IM would degrade the PUE's SE, which may even exceed the contribution of IM. When both $\bar{\gamma}$ and η are low, $P_{T_0}^e$ and $P_{T_1}^e$ are small compared to the noise. As is shown in Fig. 7(a), DIN and complete IN overlaps with non-IM, outputting slightly better SE than the other IM methods under low η. This is because at low η complete IN is not available hence is replaced by non-IM, whereas for DIN, μ^* is selected approximately 0, hence approaching non-IM. As η increases, the probability that PBS can fully neutralize the interference grows, enhancing SE. Thus, when $\eta > 20$ complete IN exceeds non-IM. Fig. 7(a) shows that DIN and adaptive IM yield almost the same SE. This can be explained by the fact that modes II and III are inferior to non-IM and IN under small $\bar{\gamma}$; besides, non-IM and complete IN are special cases of DIN, thus making adaptive IM essentially equivalent to DIN. Specifically, the adaptive IM prefers non-IM when η is small and employs complete IN for large η, whereas for DIN, $\mu^* = 0$ is adopted when η is

small which is equivalent to non-IM, when η becomes large complete IN outperforms non-IM, so DIN adopts $\mu^* = 1$.

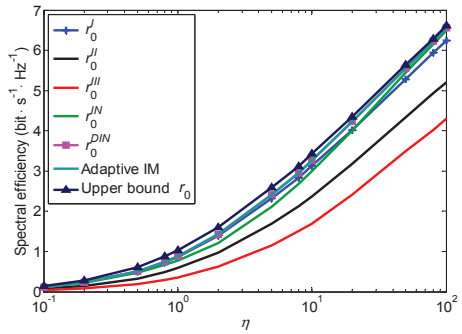

(a) $\bar{\gamma} = -5dB$.

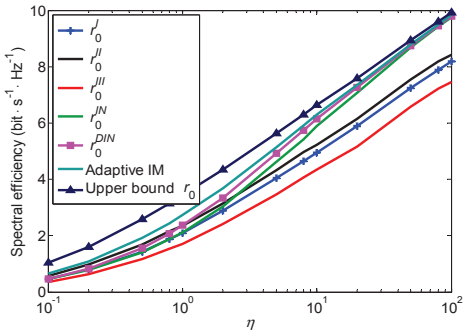

(b) $\bar{\gamma} = 5dB$.

Fig. 7. Spectral efficiency of PUE vs. η with various IM schemes under $N_{T_0} = N_{R_0} = N_{T_1} = 2$ and different $\bar{\gamma}$.

Fig. 7(b) shows the case when the interference is relatively stronger than noise. IM contributes more to SE enhancement. Especially for ZF, its achievable SE is higher than that of non-IM. When η is high or extremely low, DIN overlaps with complete IN, whereas for the other η values, DIN is superior to IN. This is because PBS is able to neutralize relatively weak interference when η is large, and hence DIN tends to become complete IN. For very small η, DIN and IN are equivalent to non-IM. With medium η, DIN could better utilize P_{T_0} for both interference neutralization and the desired signal's transmission. As a result, DIN's overall SE performance is better than that of complete IN.

TABLE III
THE PREFERRED IM SCHEME UNDER EXTREME η AND $\bar{\gamma}$.

$\bar{\gamma}$ \ η	Low	High
Low	DIN (non-IM)	DIN (Complete IN)
High	ZF	DIN (Complete IN)

Based on Figs. 6 and 7, the method that adaptive IM selects with a high probability under extreme η and $\bar{\gamma}$ combinations is shown in Table III. Since DIN subsumes complete IN and non-IM as special cases, and ZF outperforms mode III, the adaptation is the choice between DIN and ZF.

VI. Conclusion

In this paper, we proposed an adaptive interference management (IM) mechanism that incorporates *dynamic interference neutralization* (DIN). The existence of an optimal portion of interference to be neutralized has been theoretically proved. Our in-depth simulation results show that DIN could achieve better use of the transmit power, enhancing spectral efficiency. Here we mainly focused on the management of a single interference and restricted DIN to the adjustment of power. In practice, however, multiple interferences may originate from one or multiple transmitters. Which interference(s) and how much of each interference should be neutralized so as to optimize the system's SE are also important issues that warrant further investigation. In order to solve these problems, both power and spatial domains should be taken into account. These are matters of our future inquiry.

Acknowledgments

This work was supported in part by NSFC (U1405255); the 111 Project (B16037, B08038). It was also supported in part by the US National Science Foundation under Grant 1317411.

References

[1] T. Yoo, A. Goldsmith, "On the optimality of multianntenna broadcast scheduling using zero-forcing beamforming," IEEE J. Select. Areas Commun., vol. 24, no. 3, pp. 528-541, 2006.
[2] D. Tse, P. Viswanath, "Fundamentals of Wireless Communication," Cambridge University Press, 2004.
[3] V. R. Cadambe, S. A. Jafar, "Interference alignment and spatial degrees of freedom for the k user interference channel," in Proc. of the IEEE Int. Conf. on Commun. (ICC), pp. 971-975, 2008.
[4] C. M. Yetis, T. Gou, S. A. Jafar, et al., "On feasibility of interference alignment in MIMO interference networks," IEEE Trans. Sig. Process., vol. 58, no. 9, pp. 4771-4782, 2010.
[5] C. Na, X. Hou, A. Harada, "Two-cell coordinated transmission scheme based on interference alignment and MU-MIMO beamforming," in Proc. of the IEEE Vehicular Technology Conf. (VTC), pp. 1-5, 2012.
[6] S. Mohajer, S. N. Diggavi, C. Fragouli, D. N. C. Tse, "Transmission techniques for relay-interference networks," in Proc. of the 46th Annual Allerton Conf. Commun., Control, Comput., pp. 467-474, 2008.
[7] J. Chen, A. Singh, P. Elia, et al., "Interference neutralization for separated multiuser uplink-downlink with distributed relays," in Proc. of the Inf. Theory and Applications Workshop (ITA), pp. 1-9, 2011.
[8] T. Gou, S. A. Jafar, C. Wang, et al., "Aligned interference neutralization and the degrees of freedom of the 2×2×2 interference channel," IEEE Trans. Inf. Theory, vol. 58, no. 7, pp. 4381-4395, 2012.
[9] S.-W. Jeon, M. Gastpar, "A survey on interference networks: Interference alignment and neutralization," Entropy, vol. 14, no. 10, pp. 1842-1863, 2012.
[10] S.-W. Jeon, C.-Y. Wang, M. Gastpar, "Approximate ergodic capacity of a class of fading 2×2×2 networks," in Proc. of the Inf. Theory and Applications Workshop (ITA), pp. 5-10, 2012.
[11] N. Lee, C. Wang, "Aligned interference neutralization and the degrees of freedom of the two-user wireless networks with an instantaneous relay," IEEE Trans. Commun., vol. 61, no. 9, pp. 3611-3619, 2013.
[12] Z. Ho, E. A. Jorswieck, "Instantaneous relaying: optimal strategies and interference neutralization," IEEE Trans. Sig. Process., vol. 60, no. 12, pp. 6655-6668, 2012.
[13] T. Q. S. Quek, G. de la Roche, M. Kountouris, "Small cell networks: deployment, PHY techniques, and resource management," Cambridge University Press, 2013.
[14] 3GPP TR 36.931 Release 12, "LTE; Evolved Universal Terrestrial Radio Access (E-UTRA); Radio Frequency (RF) requirements for LTE Pico Node B," 2014.
[15] N. C. Ericsson, "Adaptive modulation and scheduling for fading channels," in Proc. of the IEEE Global Telecommunications Conf. (Globecom), vol. 5, pp. 2668-2672, 1999.
[16] Z. Li, X. Dai, K. G. Shin, "Decoding interfering signals with fewer receiving antennas," in Proc. of the IEEE International Conf. on Computer Commun. (INFOCOM), pp. 658-666, 2016.
[17] D. Lopez-Perez, I. Guvenc, G. de la Roche, et al., "Enhanced inter-cell interference coordination challenges in heterogeneous networks," IEEE Wireless Commun. Mag., vol. 18, no. 3, pp. 22-30, 2011.